

**Infrared Imaging of the Bipolar  
Planetary Nebula M2-9 from SOFIA,  
with NGC7027 for Dessert**

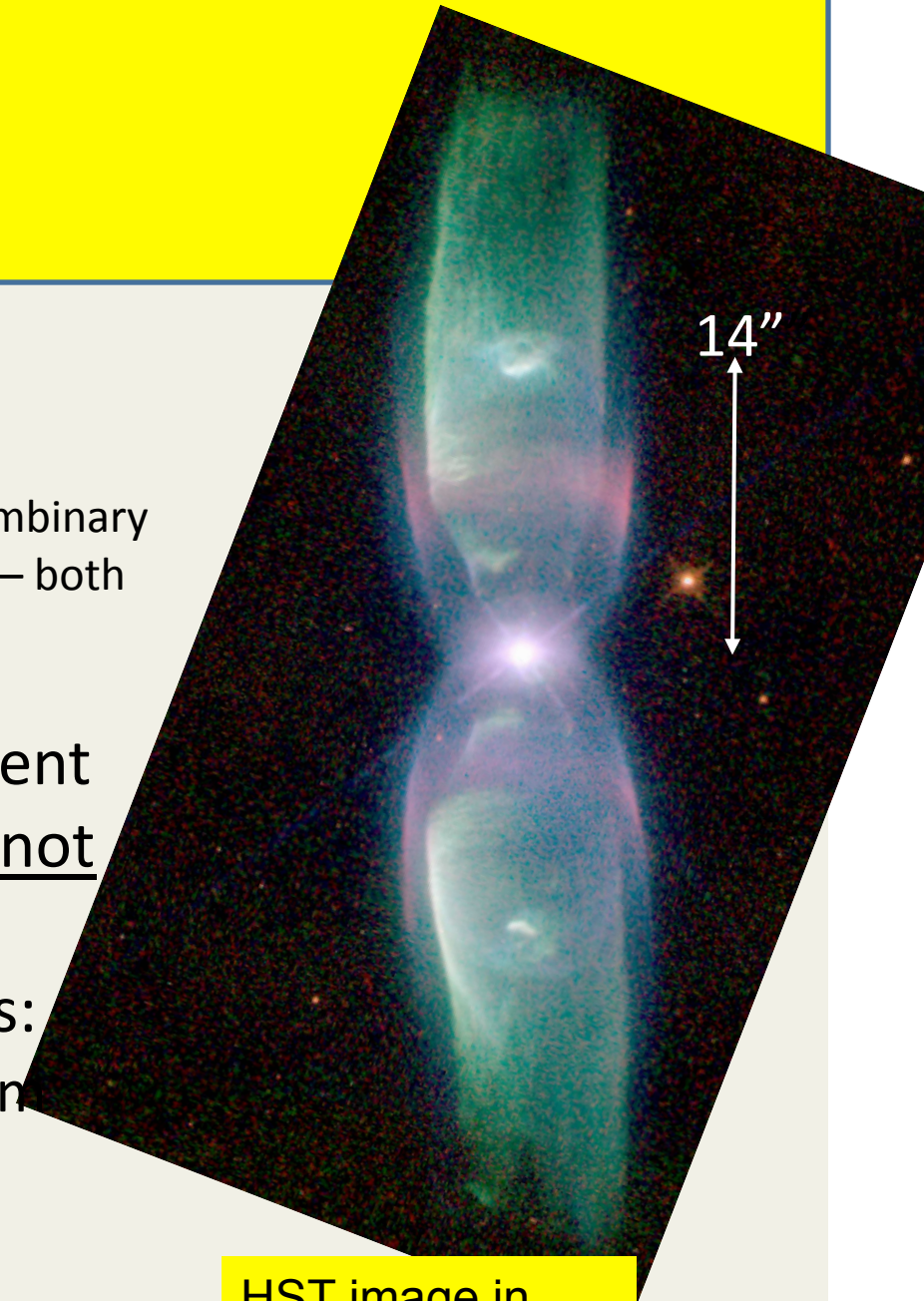
**Michael Werner, JPL/Caltech, et al  
Presented 8 May 2013**

# Compact Planetary Nebula are ideal initial targets for FORCAST:

- Bright in the infrared – often too bright for Spitzer
  - infrared emission known to peak in the 30um region
- Well matched in size to FORCAST 3.2 arcmin field of view
- Werner, Morris and Sahai were awarded 4 hours of SOFIA time to observe four such targets:
  - NGC7027, M2-9, NGC6543, Frosty Leo
- Ought also to be prime targets for GRISM spectroscopy from SOFIA

# Minkowski 2-9 is a Classic bipolar nebula

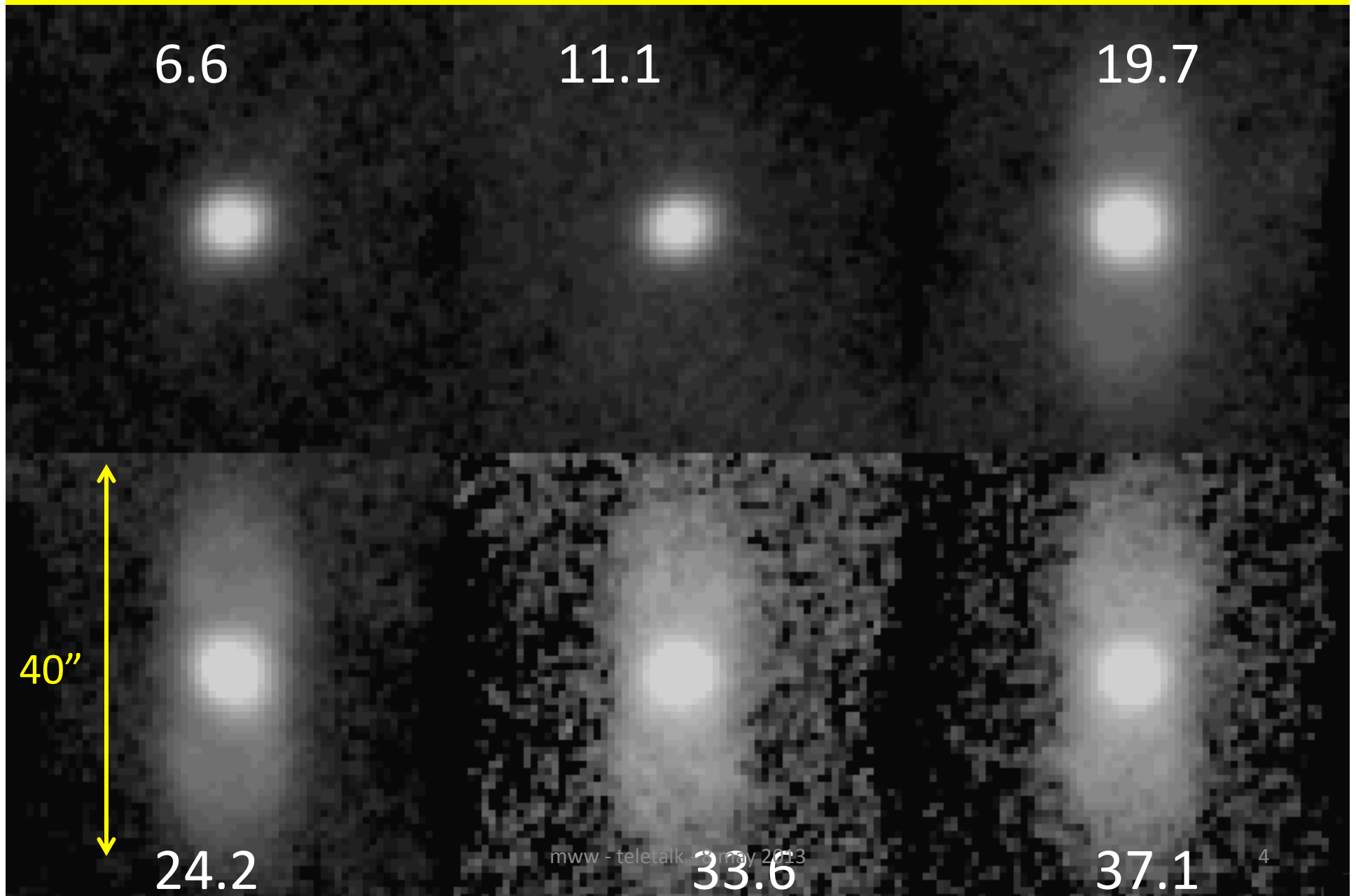
- We estimate  $L=2500 L_{\text{sun}}$ 
  - ❖ Stellar temperature 5000K
  - ❖ Powered by an AGB star/white dwarf binary
  - ❖ IR interferometry shows compact dense circumbinary central disk; CO data show two disks within  $\sim 6''$  – both perpendicular to lobes
  - ❖ High degree of temporal variability
- Distance = (1.2 Kpc). L and D consistent with model presented here. Results not critically dependent on distance
- Observed with FORCAST in six bands:
  - 6.6, 11.1, 19.7, 24.2, 33.6, 37.1  $\mu\text{m}$
  - 6-to-10 min per filter
- Photometry done on SOFIA Science Center Level 3 data products



HST image in emission lines

# SOFIA Images of M2-9

Observations: 11 May and 2 June, 2011. Chop and nod 30" EW to keep image on array continually. Approximately 10 mins/filter. Reduction by SOFIA Science Center.



# Abstract of Paper Summarizes Results

ABSTRACT. We have imaged the bi-polar planetary nebula M2-9 using SOFIA's FORCAST instrument in six wavelength bands between 6.6 and 37.1  $\mu\text{m}$ . A bright central point source, unresolved with SOFIA's  $\sim 4''$  beam, is seen at each wavelength, and the extended bipolar lobes are clearly seen at 19.7  $\mu\text{m}$  and beyond. The photometry between 10 and 25  $\mu\text{m}$  is well fit by a model of the type previously proposed for this source by Lykou et al and Chesneau et al. The principal new results in this paper relate to the distribution and properties of the dust that emits the infrared radiation. In particular, a considerable fraction of this material is spread uniformly through the lobes, although the dust density does increase at the sharp outer edge seen in higher resolution optical images of M2-9. The dust grain population in the source is unusual in that small ( $< 0.1 \mu\text{m}$ ) and large ( $> 1 \mu\text{m}$ ) particles appear to be present in roughly equal quantities (by mass). We suggest that collisional processing within the bipolar outflow plays an important role in determining the particle size distribution.

# North-South Scans, averaged over 5 pixels East West

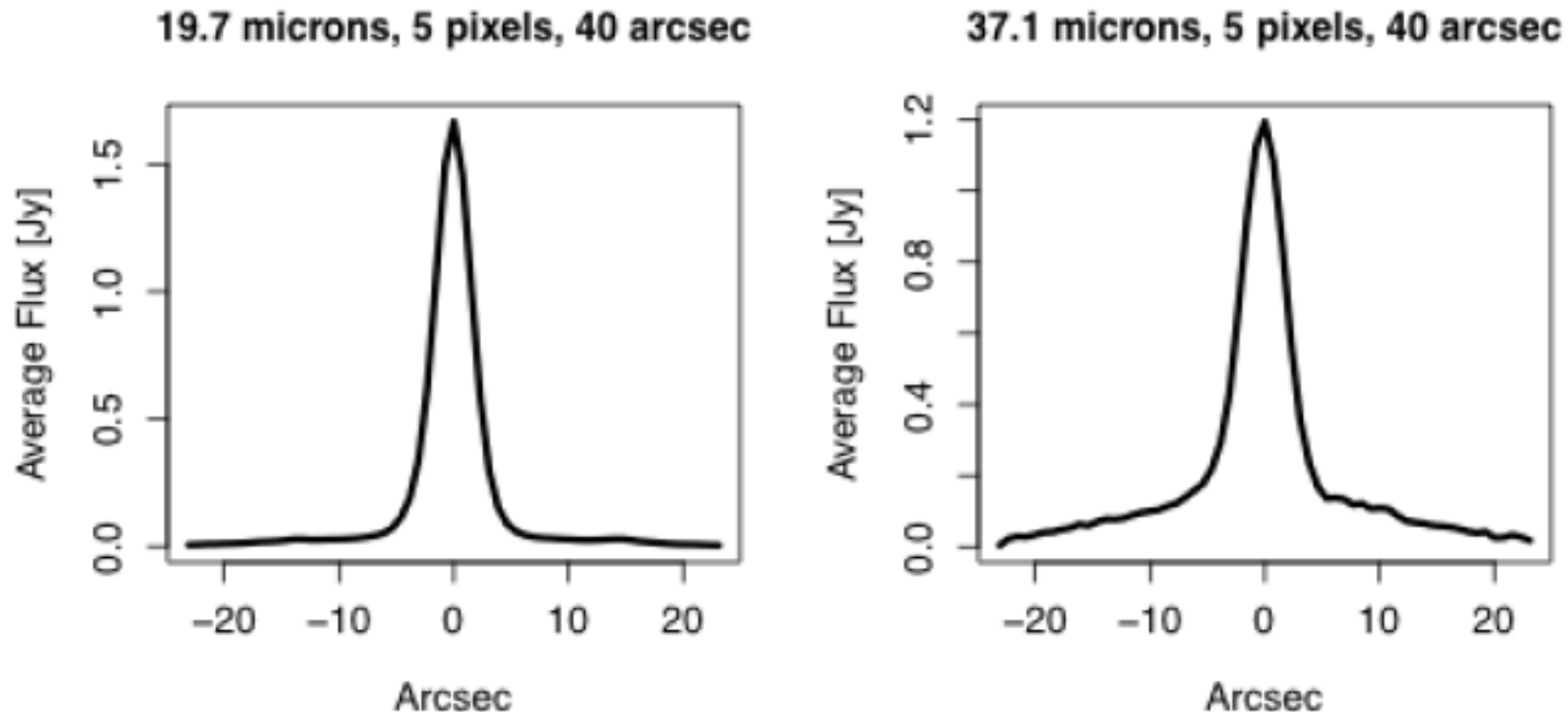


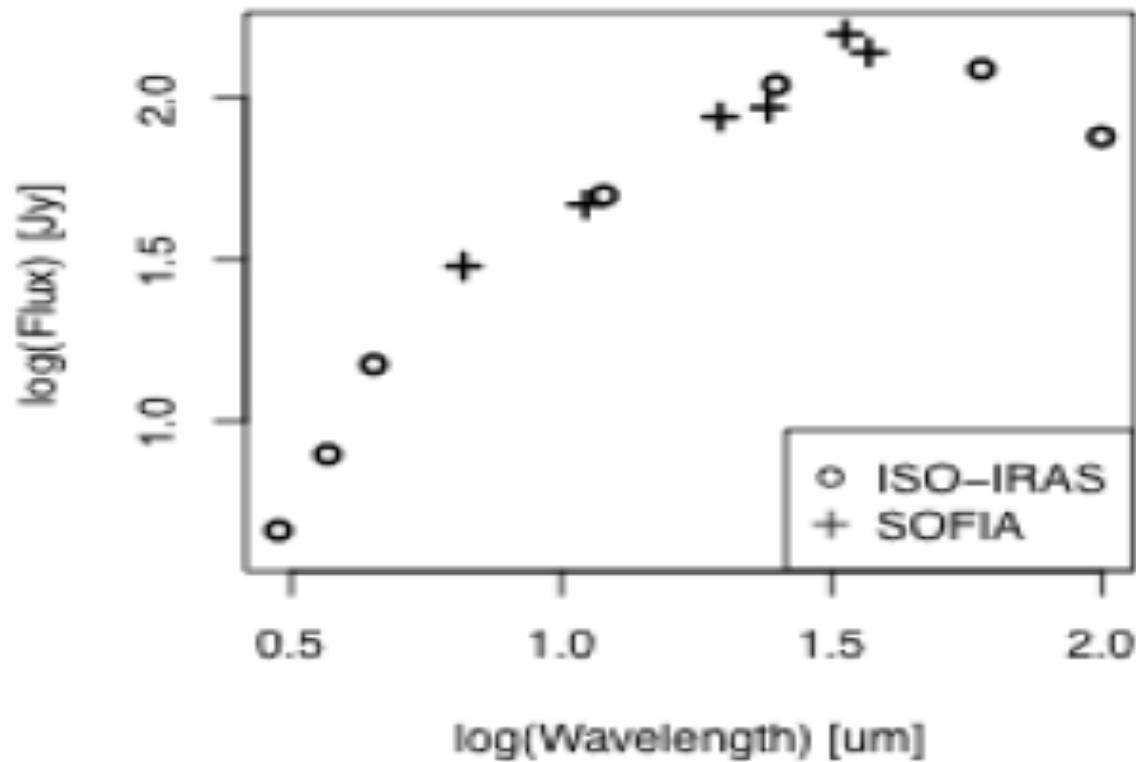
Figure 2. North-South scans at 19.7 and 37.1 microns through the central point source in M2-9

**TABLE 1. M2-9 PHOTOMETRY AND SIZE DATA**  
 [includes data from ISO, IRAS, and

[				Point Source	
Wavelength		FLUX in JY		fwhm	beam size
um	point source	total Flux [20x40"]	extended component	arcsec	arcsec*
3	4.6				
3.7	7.9				
4.5	15				
6.6	24	30.2	6.2	3.7	3.68
11.1	32	46.9	14.9	3.7	3.85
19.7	58	87.5	29.5	3.9	3.76
24.2	55	93.4	38.4	4.1	4.19
33.6	63	157.7	94.7	4.5	4.42
37.1	48	138.4	90.4	4.9	4.51
12		50			
25		110			
60		123			
100		76			
1300	0.21	0.36	0.15		

mww - teletalk - 8 may 2013

# 2.5-120 $\mu$ m SED of M2-9



## OBSERVED LUMINOSITIES

Central point source, 2.5-to-40 $\mu$ m, is  $840 L_{\text{sun}}$

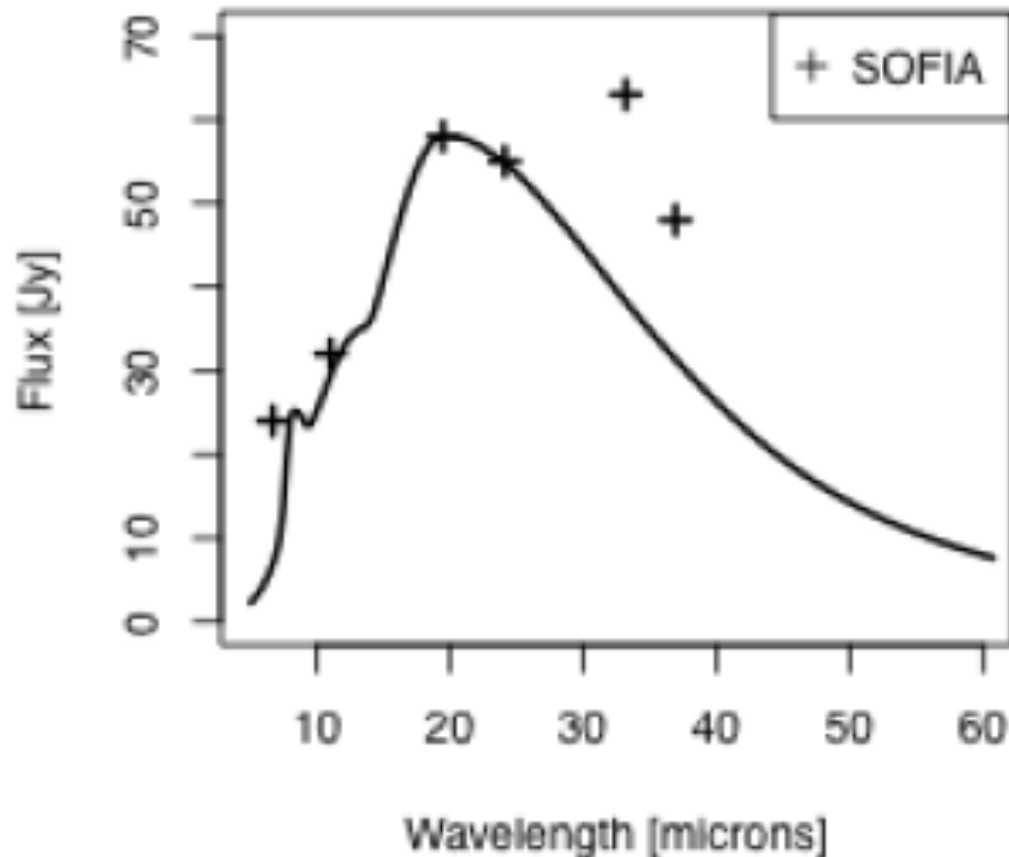
Lobes are  $390 L_{\text{sun}}$  over this wavelength range

Total, including IRAS, from 2.5-to-120 $\mu$ m, is  $1530 L_{\text{sun}}$

These estimates assume isotropic emission, which is almost certainly not the case.



# SOFIA measurements of the M2-9 point source compared with model predictions based on Lykou et al 2012



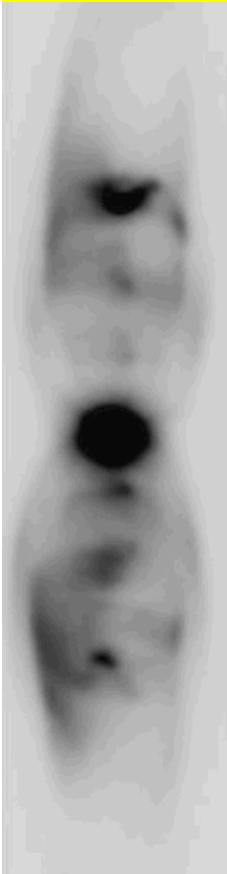
Fit is excellent over peak of emission from model. Deviations longward and shortward understandable in terms of limitations of model

# Parameters of Model Fit

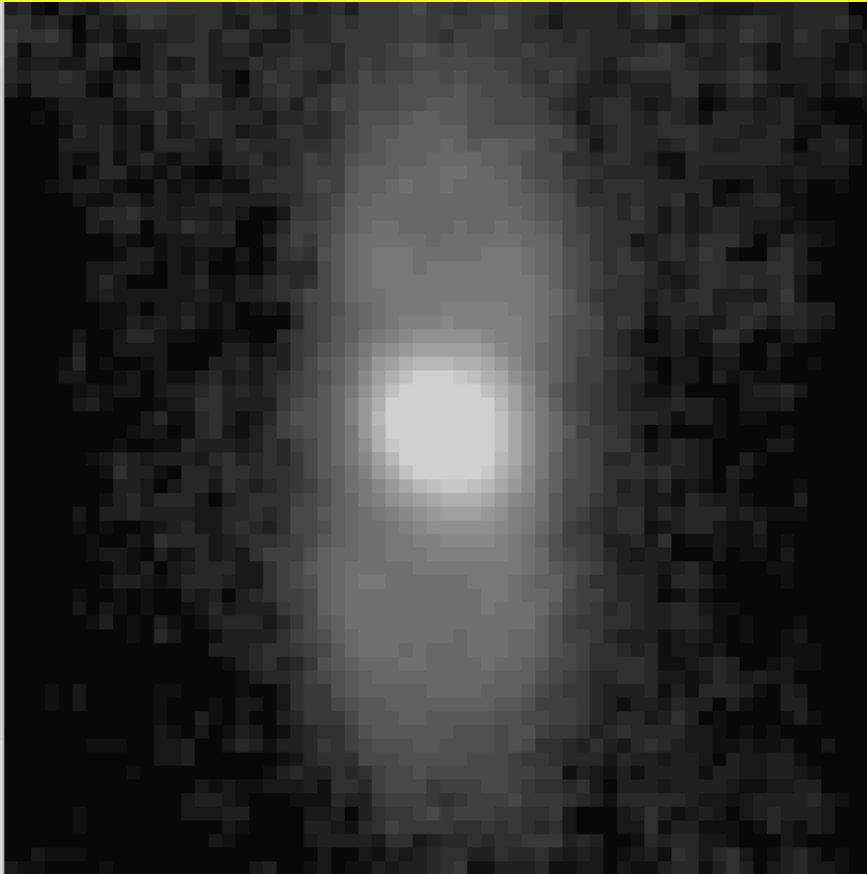
Parameter	Value	Comment
Disk inner radius	15+/-1 au	
Disk outer radius	800+/- 100 au	radius is less than 1 arcsec at best fit distance of ~1100-1250pc. We adopt 1200 pc.
Mass of dust	1+/-0.1 e-5 solar masses	Draine and Lee astronomical silicates, sizes 0.01-to-5um. Mathis et al size distribution
Alpha	2.2+/- 0.05	Density within disk falls radially as $r^{-\alpha}$
Beta	1.23+/- 0.02	Scale height varies radially as $r^{\beta}$ . Disk is flared
h_100	37 +/- 3 au	Fiducial scale height at 100 au
T_eff	5000K	Temperature of AGB star doing most of the heating
L	2500 Lsol	Luminosity of AGB star

Our measurements give 1530 solar luminosities for the nebula, less than the 2500 implied by the model; however, the emission is undoubtedly asymmetrical, with more power going perpendicular to the disk in the plane of the sky, and the lobes do not have high radial optical depth, so that some of the heating radiation escapes.

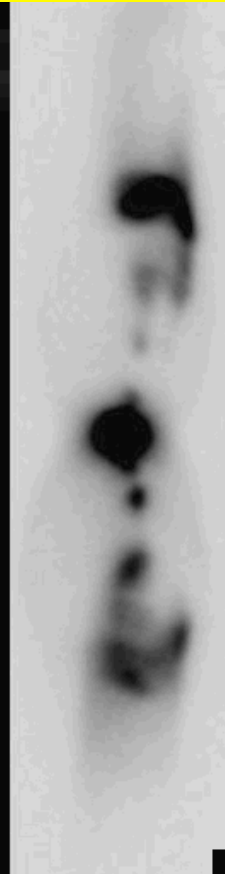
# Turning to the Lobes



H $\alpha$ + [NII]  
(2010)



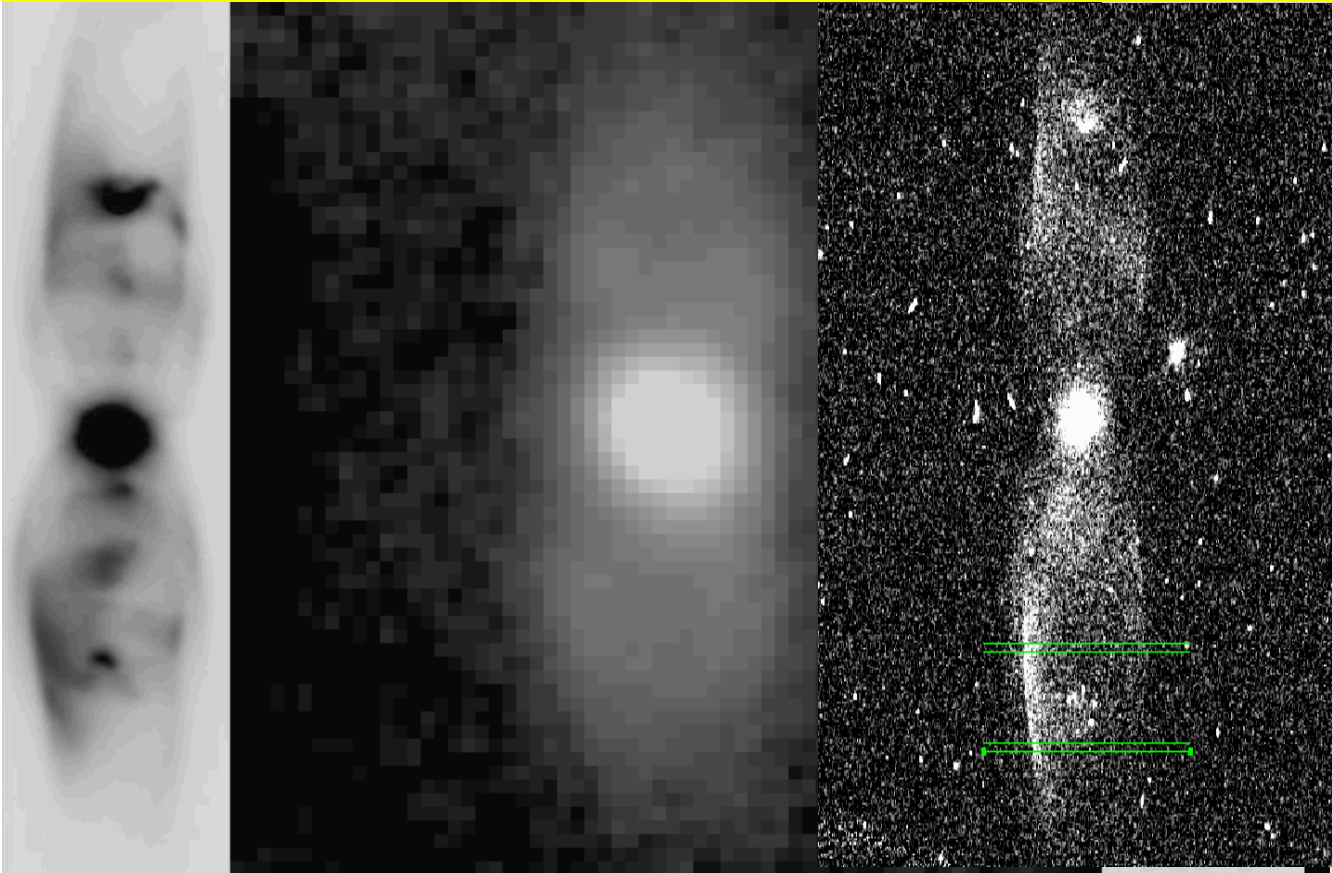
24.2 $\mu$ m



[OIII]  
(2010)

- Infrared emission comes from region comparable in size to that seen in the optical
- Lobes show structure and limb brightening in visible
- Distribution smoother in the infrared, although some structure is seen
- Difference in spatial resolution partly, not totally responsible
- We attribute the radiation to emission from dust; gas phase lines are seen but not that strong

# Turning to the Lobes, II



Halpha+[NII]  
(2010)

24.2um

547nm  
continuum (1997)

- Infrared emission comes from region comparable in size to that seen in the optical
- Lobes show structure and limb brightening in visible
- Distribution smoother in the infrared, although some structure is seen
- Difference in spatial resolution partly, not totally responsible for this

# Implications of Lobe Emission

## The SED

- Lobe emission peaks around 35-40 $\mu\text{m}$ , corresponding to a grain temperature of  $\sim 100\text{K}$
- Grey or black particle  $\sim 10''$  from the central source at the distance of M2-9 would have  $T \sim 20\text{K}$ .
- Conclusion: Infrared radiation from lobes comes from small particles. We have modelled this as  $\sim 0.1\mu\text{m}$  radius amorphous carbon particles. This fits reasonably over the wavelengths of

peak power emission. The implied mass of small particles is  $\sim 0.001 M_{\text{sun}}$

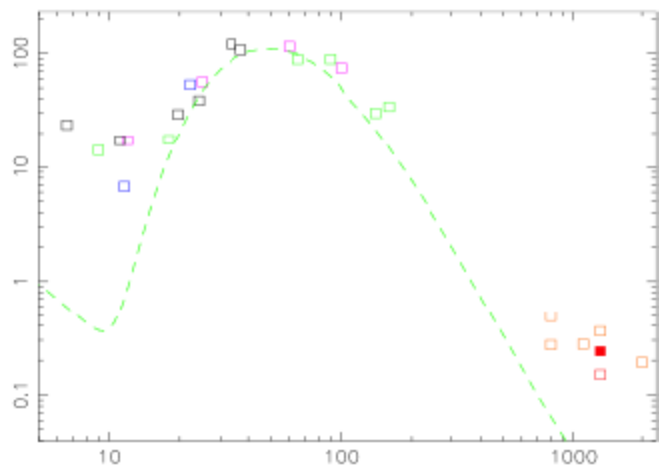


Figure 5. Model fit to the extended emission from M2-9

# But wait, there's more!....

- SED's shown previously provide reasonably good fits to emission from both the lobes and the central compact source, but....

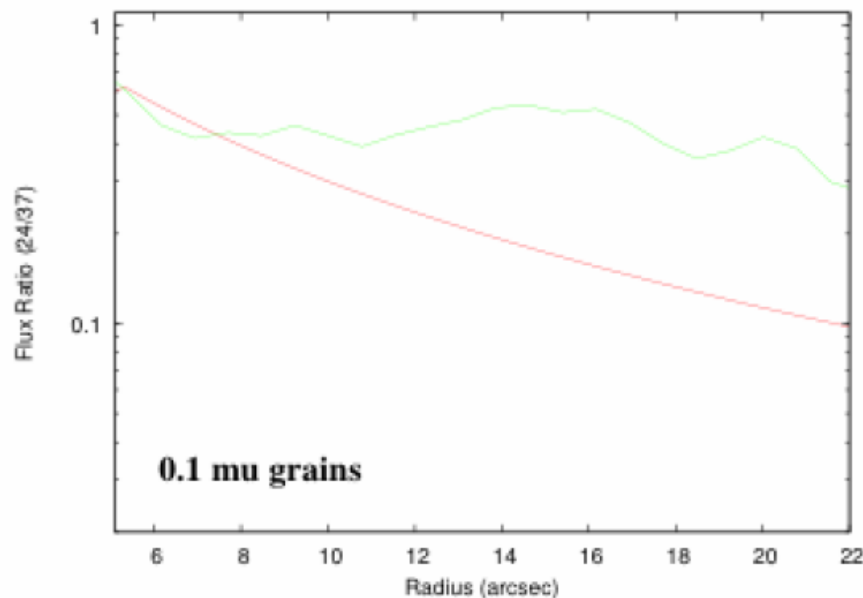
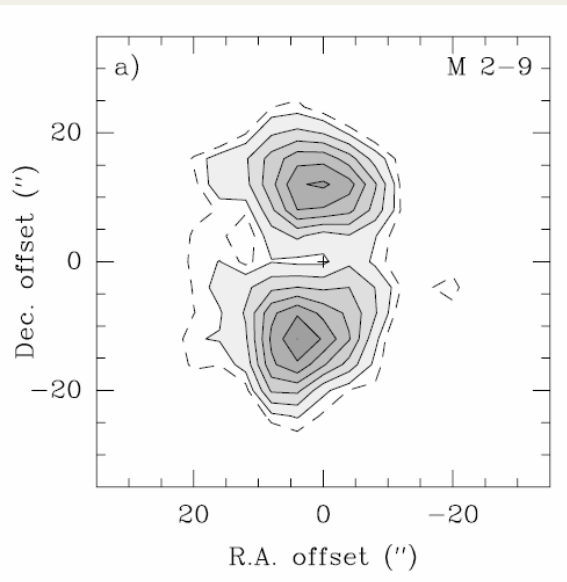


Figure 6. Variation of 24/37um flux ratio as a function of distance North of the M2-9 point source, based on the model shown in Figure 5. Data are in green, model prediction in red.

- As shown to the left, the 24/37um flux ratio as a function of position does not agree well with the data.
- Farther than  $\sim 10''$  from the central source the ratio no longer decreases with distance, as it should if the grain temperature continues to drop
- We interpret this as due to the fact that at this point, single photon heating of the small particles becomes dominant. The ratio would then be distance-independent
- This is roughly consistent with the observation of single photon heating out to  $\sim 25\mu\text{m}$  within a few arcminute of 23 Tau in the Pleiades.

# ...and Yet More!

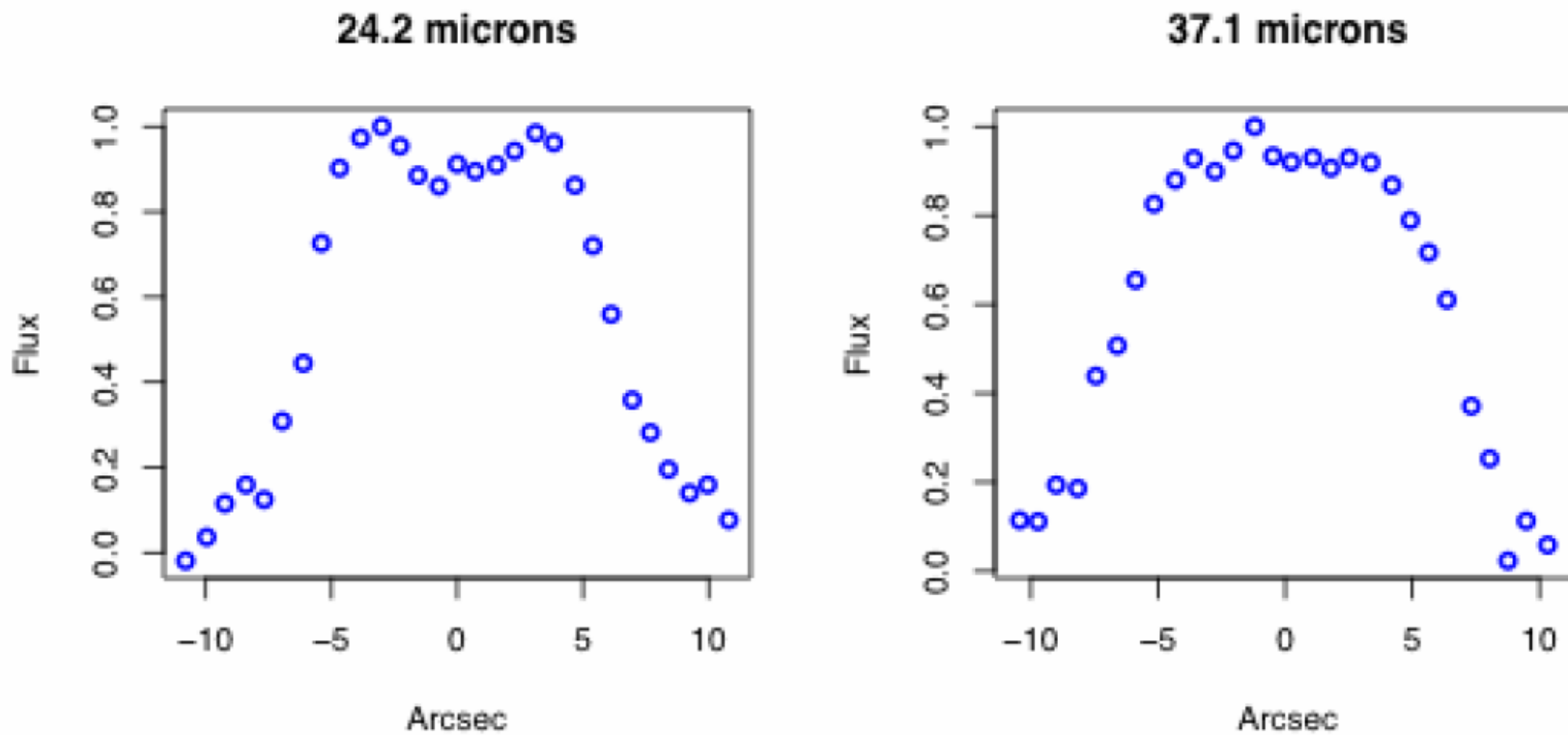


1.3mm extended emission from M2-9, after point source is subtracted

- At 1.3mm, M2-9 shows both a central point source and extended emission from the lobes
- It appears that the lobe emission is best interpreted as thermal emission from dust, as opposed to some form of free-free emission
- This requires particle sizes  $>1\mu\text{m}$ , as opposed to the much smaller particles producing the emission seen in the lobes
- Sanchez-Contreras et al estimate a particle mass of  $\sim 0.0015 M_{\text{sun}}$  in these large particles if they are composed of amorphous carbon.
- In addition, both they and Castro-Carrizo et al measure strong 1.3mm emission from the central point source, suggesting that it also contains large particles in substantial number
- Note that the mass of large particles is comparable to the mass of small ones

# Modelling the Dust Distribution

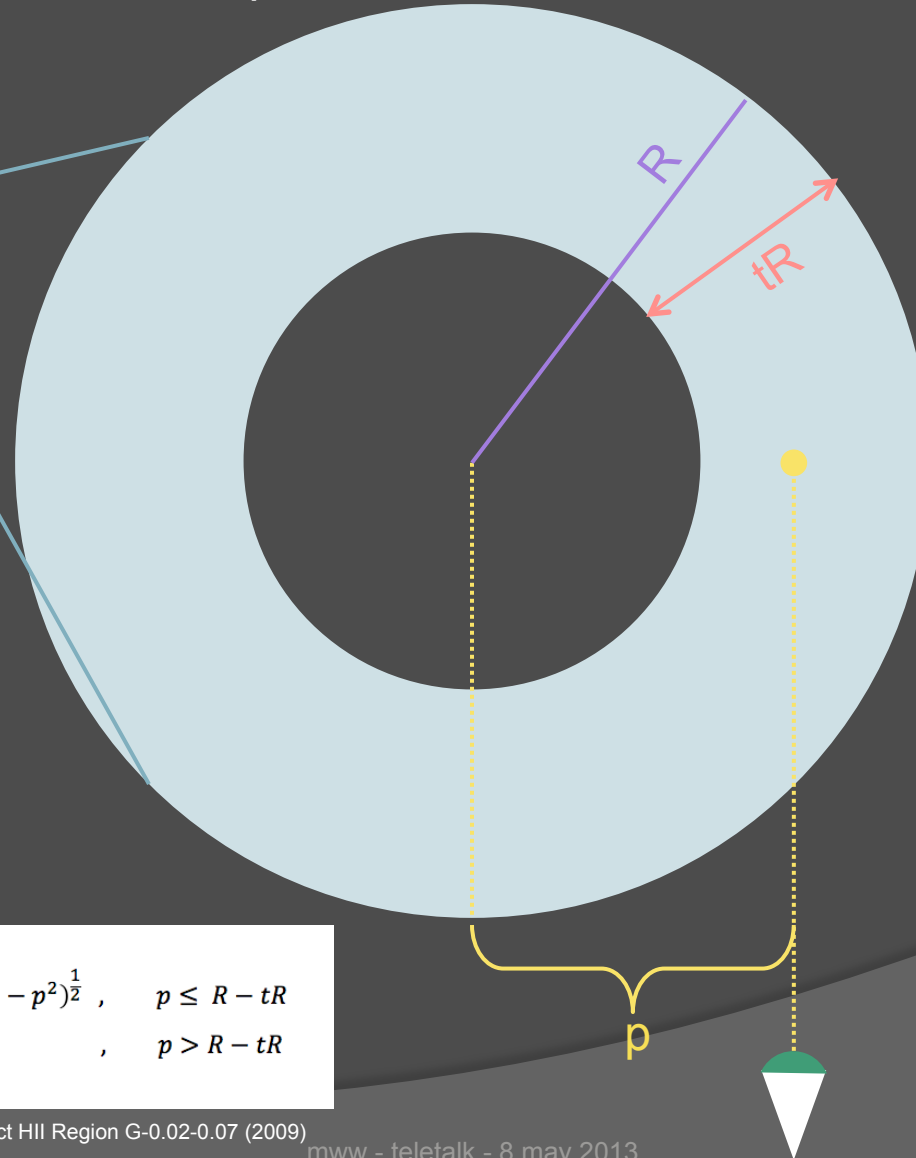
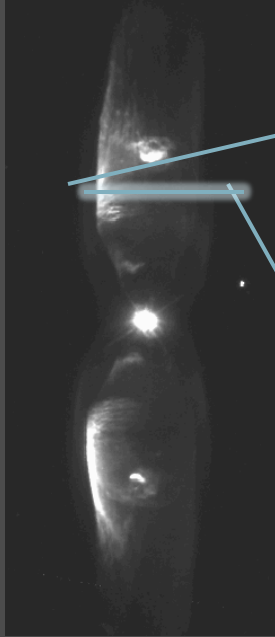
- The figure below shows E-W scans through the northern lobe at a position 10" N. of the central source, averaged over 3 pixels in the N-S direction.





# Modeling Lobe Structure

Cylinder radius is 6" 10" N of point source, based on HST.



We consider uniform annular emissivity distributions, parameterized by a factor  $t$ .  $t=1.0$  corresponds to a uniformly filled cylinder, while  $t=0.05$  is a cylinder which is largely empty with material only in the outer 5%. Compare model to scans at 37.1 $\mu\text{m}$ , to justify neglect of temperature variations. Use a one-dimensional Gaussian approximation to the telescope beam for initial exploration

Model

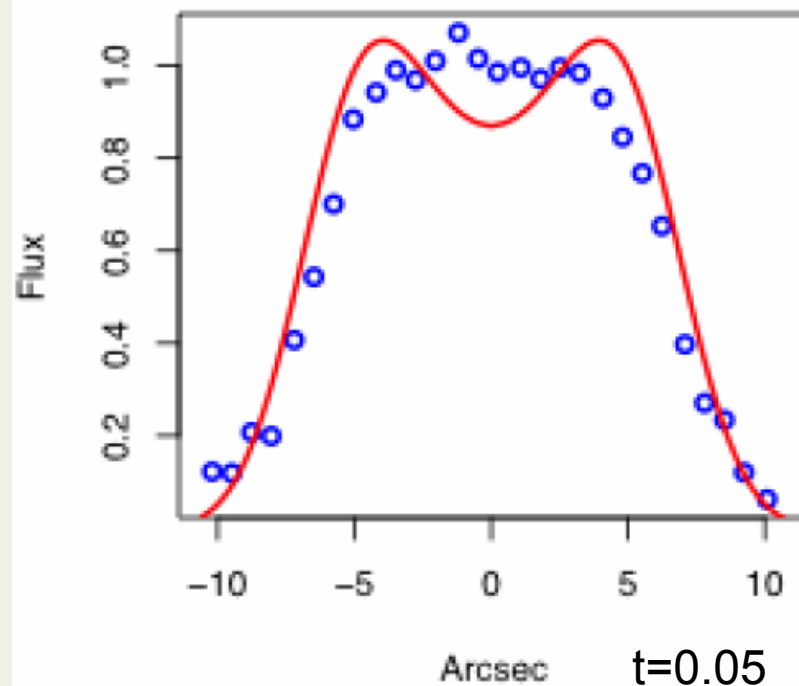
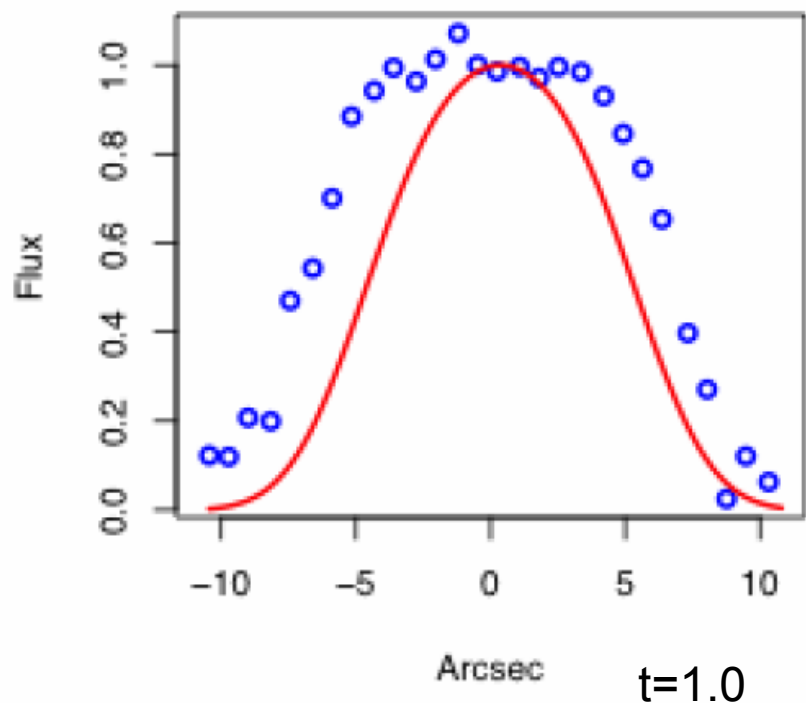
$$L(p) = 2 \begin{cases} (R^2 - p^2)^{\frac{1}{2}} - ((R - tR)^2 - p^2)^{\frac{1}{2}}, & p \leq R - tR \\ (R^2 - p^2)^{\frac{1}{2}}, & p > R - tR \end{cases}$$

From Morris et al. Properties of the Compact HII Region G-0.02-0.07 (2009)

mww - teletalk - 8 may 2013

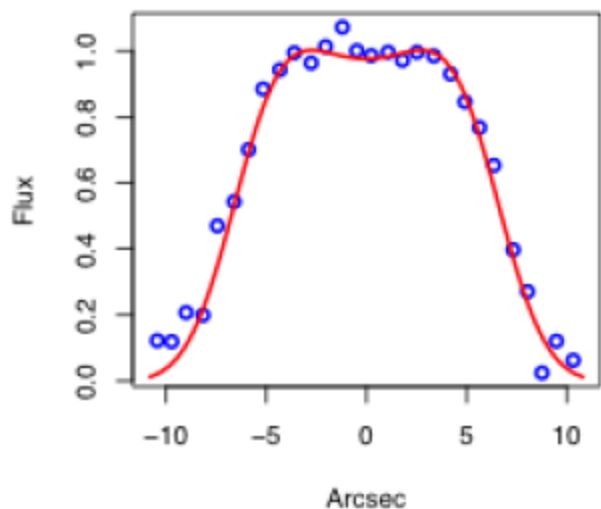
# Two Limiting Cases

[model in red, data in blue]



Neither the uniform filled cylinder ( $t=1.0$ ) nor the extremely limb-brightened one ( $t=0.05$ ) provides a good fit to the scan at  $37.1\mu\text{m}$   $10''$  N. of the center. These results motivated us to examine a simple linear combination of these two cases.

# A Good Fit....



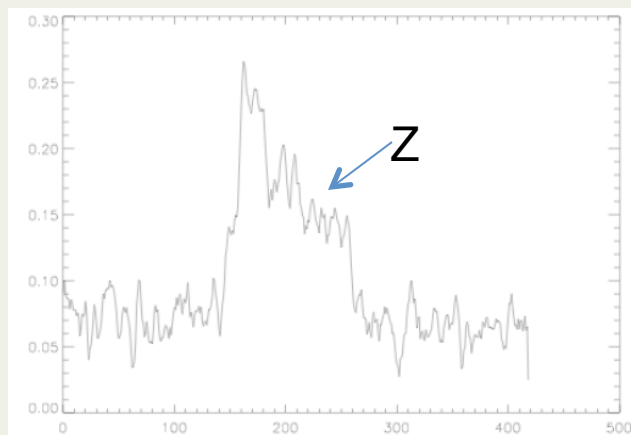
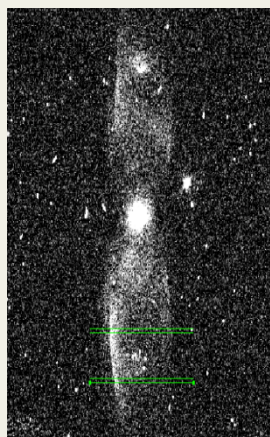
A good fit is provided by a model which has 30% of the dust in a uniform [ $t=1$ ] distribution and 70% at the limb of the lobe [ $t=0.05$  or less].

Note that we have only two-or-three resolution elements across the lobe. So this is not a unique fit...in particular, the  $t=1$  distribution could fall off to the center of the lobe, and/or the material at the limb could be external.

The model with an interior increase at the edge of the lobe could be consistent with the high degree of limb brightening seen in some of the optical emission lines.

Basic conclusion, which is that an appreciable fraction of the infrared emission comes from within the lobe, is well established.

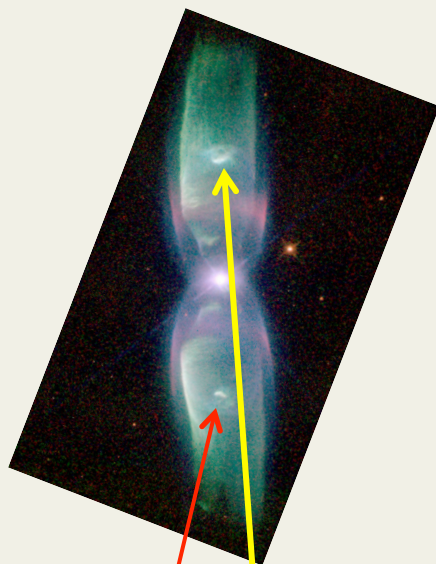
# ...but Wait, There's More.....



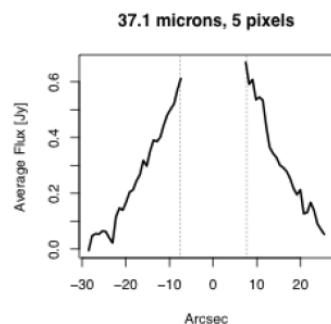
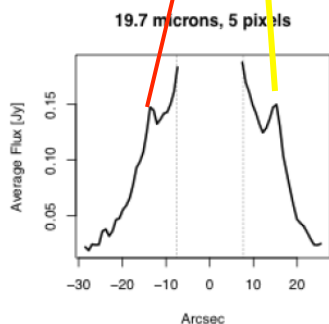
547 nm continuum image and scan 10"N shows substantial brightening of Eastern limb. We believe that the radiation at this wavelength is scattered starlight

- We assume that the bright Eastern limb is a persistent feature from 1997 to 2011
- The degree of limb brightening seen in the visible images would have been obvious in the infrared data, even if the bright spot rotated partway around the lobe in the 14 years between the visible and IR measurements
- The scattered light in region Z to the West of the limb has about 2% of the power of the infrared emission from this region, implying low grain albedo.
- We suggest that, given the broad grain size distribution in this source, that a small admixture of larger, higher albedo grains at the limb of the lobe could produce the scattered light without much of an influence on the re-emission.
- Above applies if heating due to starlight – isotropic or beamed. If the limb is excited by a particle beam, situation is more complex

# ....and Just a Tad More



- The knots in the lobes about 15" N and S of the central source are persistent features of M2-9.
- They may be compressed and excited by energetic outflow[s] from the central source.
- These are clearly seen at 19.7  $\mu\text{m}$  in long scans through the central source
- Not obvious at 37.1  $\mu\text{m}$



- Tempting to attribute this emission to line emission in the 19.7  $\mu\text{m}$  band, particularly as 18.7  $\mu\text{m}$  [SIII] line in this filter is strong in Spitzer spectrum
- However, line too weak by at least 10x to account for the emission.
- Suggest that emission might be due to heating or modification of the grains in these knots by high velocity outflows which excite the visible emission

# Observational Conclusions

- At wavelengths from 6.6 to 37.1 $\mu\text{m}$ , the image of M2-9 is dominated by a bright central point source, which is not definitely resolved at any wavelength with SOFIA's ~4-to-5" beams.
- The extended bipolar lobes are clearly seen at wavelengths from 19.7 to 37.1 $\mu\text{m}$ ; the integrated emission from the lobes is detected down to 6.6 $\mu\text{m}$ .
- The infrared emission of the point source at wavelengths between 11.1 and 24.2 $\mu\text{m}$  agrees extremely well with the predictions of the disk model of Lykou et al (2011). The fit suggests a distance of 1200 pc to M2-9 and a luminosity of 2500  $L_{\text{sun}}$  for the post-AGB star which powers it. Our principal results do not depend critically on the adopted distance or luminosity, however.
- The bright optical knots seen ~15" North and South of the central source are seen at 19.7 but not 37.1 $\mu\text{m}$ . The emission is too bright in the infrared to be due to emission lines but may result from grain heating or processing by energetic outflows.

# Conclusions of Interpretation

- Unusually, grains of sizes  $<0.1\mu\text{m}$  and  $>1\mu\text{m}$  in radius are present with comparable masses. This is in marked contrast to single power law distribution usually adopted. We suggest that large grains from the central source and/or the molecular disk are levitated in a disk wind, and that the smaller grains are produced by grain-grain or gas-grain collisions in the dynamic environment of this source. The grain population is not in collisional equilibrium, which is consistent with the short dynamical time scales which characterize this source.
- Modelling of EW scans through the northern lobe  $\sim 10''$  N of the central source show that:
  - *A significant fraction [ $\sim 30\%$ ] of the emission comes from material which is smoothly distributed throughout the lobe.*
  - *The remainder can be attributed to increased emission arising at the edge of the lobe, perhaps related to the limb brightened visible wavelength emission lines*
  - *The scattered visible wavelength light at the western side of the lobe is produced by grains with very low effective albedo. A relatively small number of larger grains could produce the limb brightened continuum emission at the eastern limb.*
- These results, plus those on NGC7027 presented next, show that SOFIA can make major contributions to our understanding of compact planetary and protoplanetary nebulae

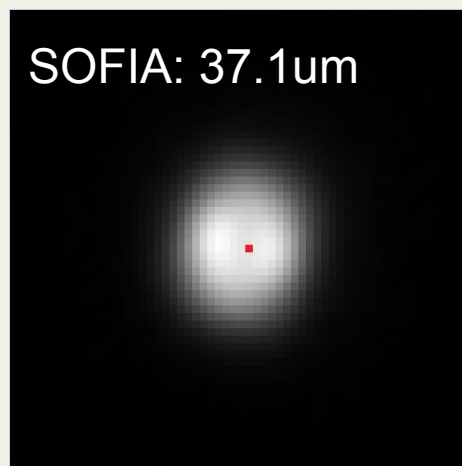
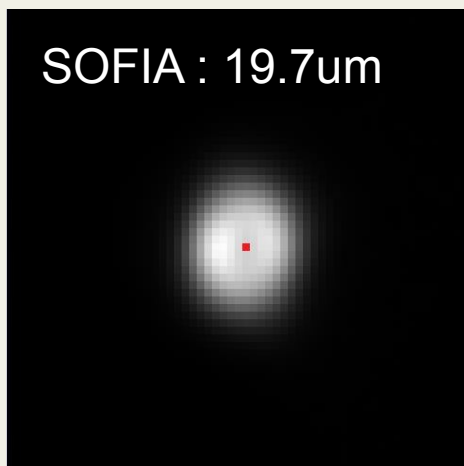
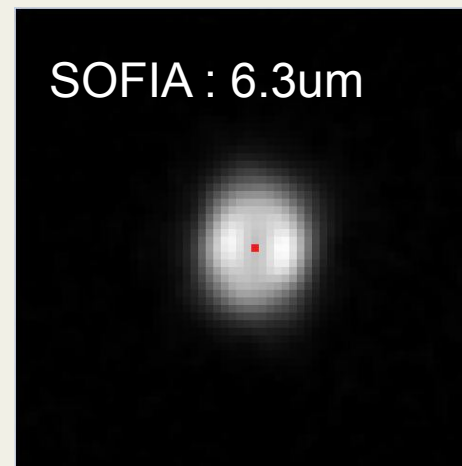
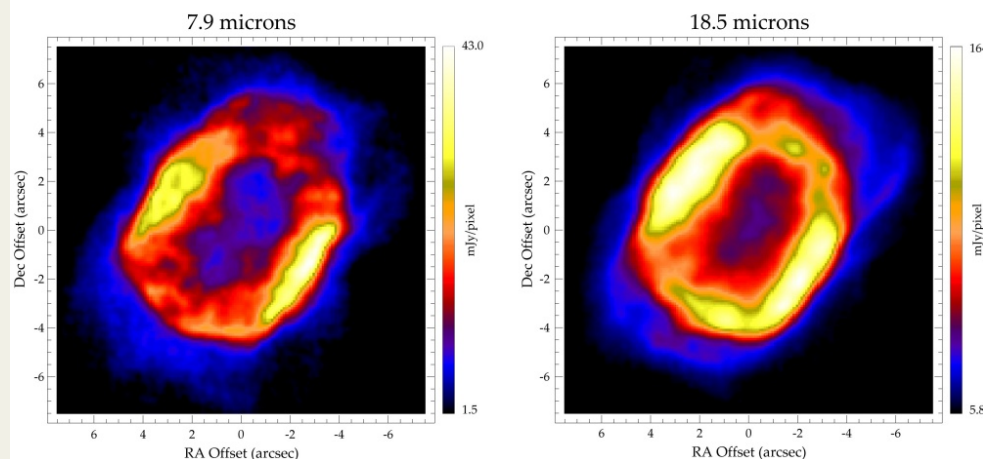
# Summary of Results on NGC7027

- During the same flight series, we observed NGC7027, everyone's favorite planetary nebula.
- NGC7027 is of the brightest and best-studied planetary nebulae. The nebula is 600pc from earth and about 0.08pc in size. It has a dynamical lifetime of only 600 yrs, making it one of the youngest known planetaries. The central white dwarf has a luminosity of  $\sim 6000 L_{\text{sun}}$  and a temperature of  $\sim 185000\text{K}$ .
- We observed NGC7027 in 7 bands, adding the 6.4um "PAH" filter to the six used for M2-9



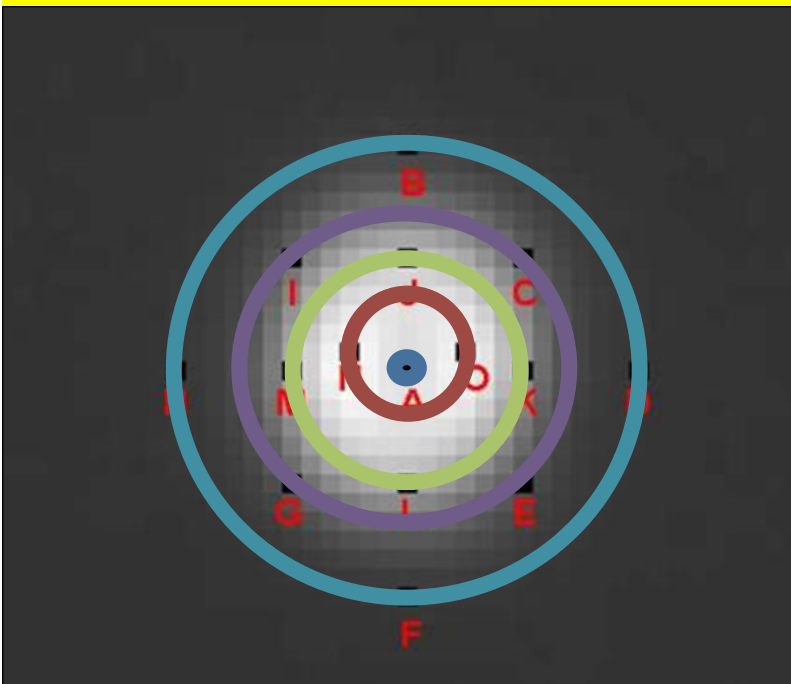
# The Structure of NGC7027 is Wavelength Independent

*Michelle Imaging of NGC 7027*

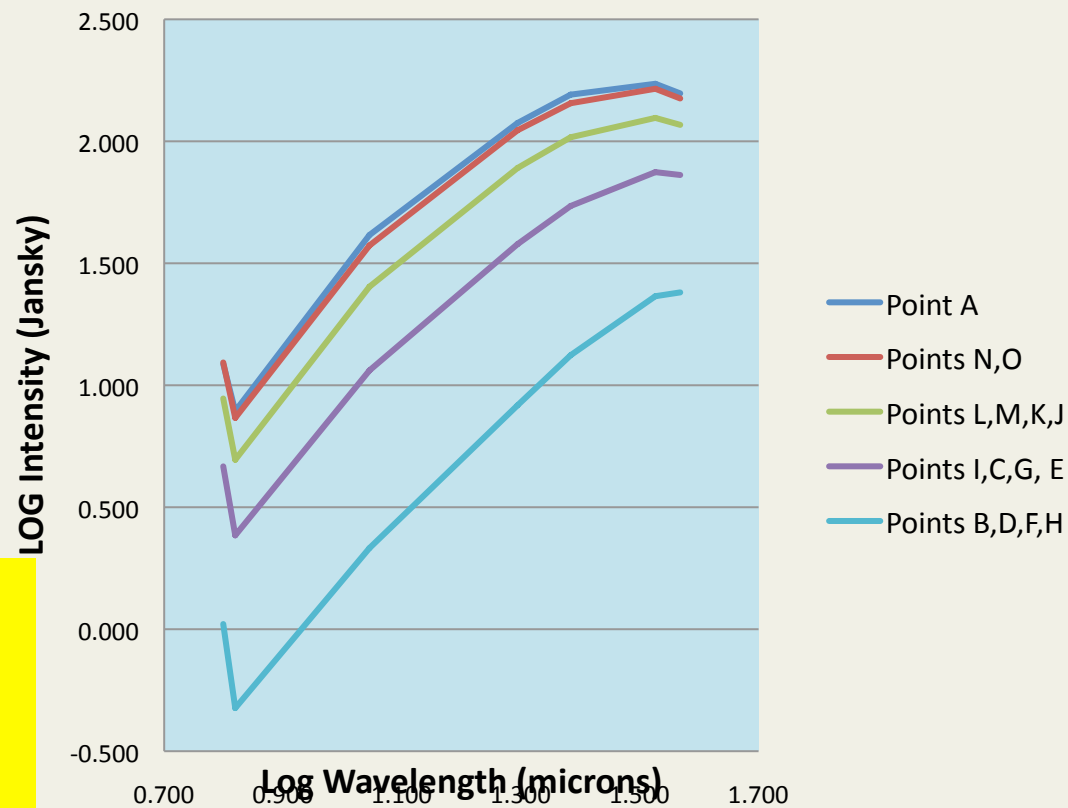


- Bearing in mind wavelength dependence of resolution, NGC7027 is very similar in morphology throughout the infrared.
- SOFIA images resemble ground-based IR and radio images as well – dust is well-mixed with ionized gas.
- No evidence for cooler, exterior shell
- PAH filter image resembles that at 6.6um

# The SED is Independent of Position

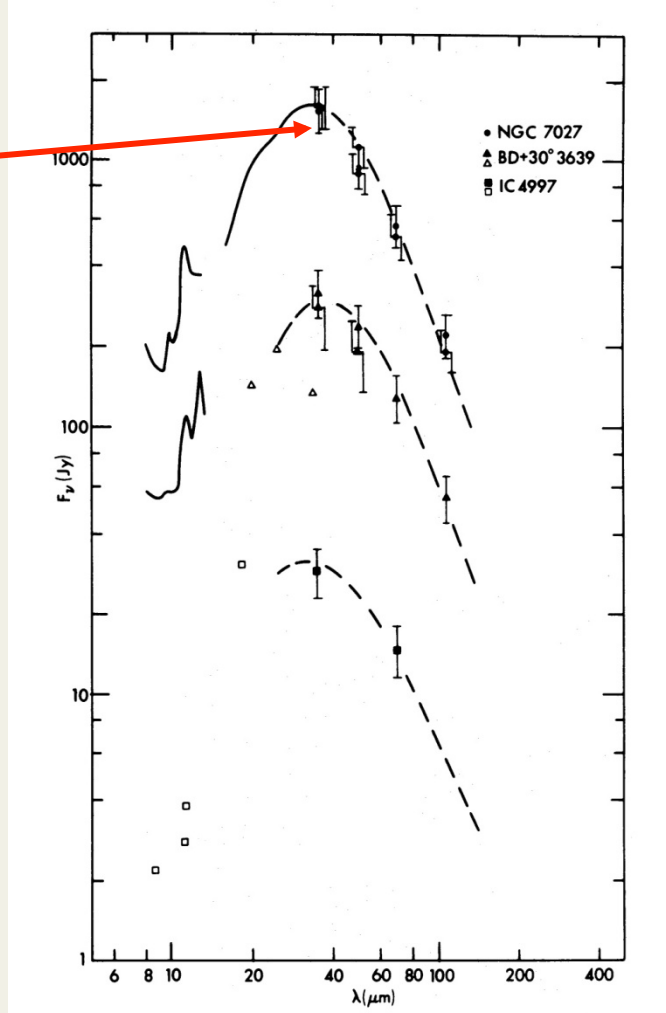
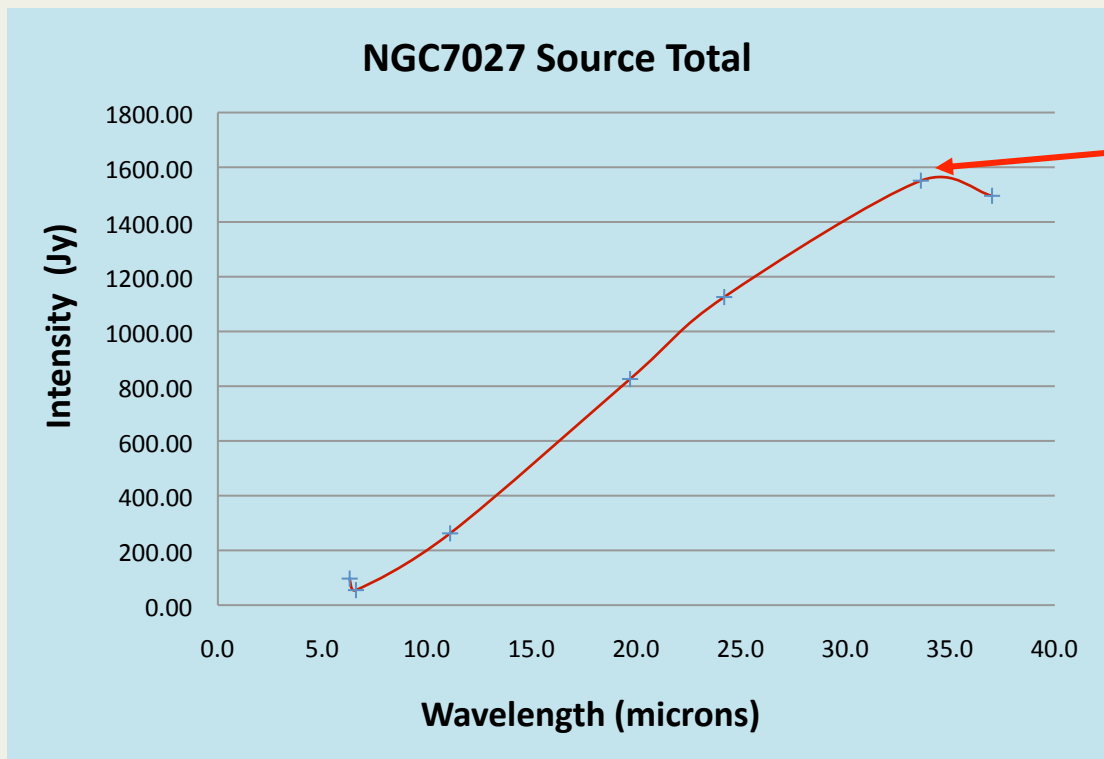


NGC7027 - SED Based on Distance from Nebula Center



- Absence of major temperature gradients consistent with heating by:
  - Trapped Lyman-alpha
  - Single photon absorption events

# SOFIA Results Consistent with Previous Photometry [also for M2-9]



Comparison of SOFIA results [above] with earlier work from KAO [right]